


ORIGINAL RESEARCH

Nitrogen control of transpiration in grapevine

Michele Faralli^{1,2}  | Pier Luigi Bianchedi³ | Claudio Moser² | Luana Bontempo² | Massimo Bertamini^{1,2}

¹Center Agriculture Food Environment (C3A), University of Trento, via Mach 1, San Michele all'Adige, TN 38098, Italy

²Research and Innovation Centre, Fondazione Edmund Mach, via Mach 1, San Michele all'Adige, TN 38098, Italy

³Technology Transfer Centre, Fondazione Edmund Mach, via Mach 1, San Michele all'Adige, TN 38098, Italy

Correspondence

Michele Faralli, Center Agriculture Food Environment (C3A), University of Trento, via Mach 1 San Michele all'Adige, TN 38098, Italy.
Email: michele.faralli@unitn.it

Edited by J. Flexas

Abstract

Transpiration per unit of leaf area is the end-product of the root-to-leaf water transport within the plant, and it is regulated by a series of morpho-physiological resistances and hierarchical signals. The rate of water transpired sustains a series of processes such as nutrient absorption and leaf evaporative cooling, with stomata being the end-valves that maintain the optimal water loss under specific degrees of evaporative demand and soil moisture conditions. Previous work provided evidence of a partial modulation of water flux following nitrogen availability linking high nitrate availability with tight stomatal control of transpiration in several species. In this work, we tested the hypothesis that stomatal control of transpiration, among others signals, is partially modulated by soil nitrate (NO_3^-) availability in grapevine, with reduced NO_3^- availability (alkaline soil pH, reduced fertilization, and distancing NO_3^- source) associated with decreased water-use efficiency and higher transpiration. We observed a general trend when NO_3^- was limiting with plants increasing either stomatal conductance or root-shoot ratio in four independent experiments with strong associations between leaf water status, stomatal behavior, root aquaporins expression, and xylem sap pH. Carbon and oxygen isotopic signatures confirm the proximal measurements, suggesting the robustness of the signal that persists over weeks and under different gradients of NO_3^- availability and leaf nitrogen content. Nighttime stomatal conductance was unaffected by NO_3^- manipulation treatments, while application of high vapor pressure deficit conditions nullifies the differences between treatments. Genotypic variation for transpiration increase under limited NO_3^- availability was observed between rootstocks indicating that breeding (e.g., for high soil pH tolerance) unintentionally selected for enhanced mass flow nutrient acquisition under restrictive or nutrient-buffered conditions. We provide evidence of a series of specific traits modulated by NO_3^- availability and suggest that NO_3^- fertilization is a potential candidate for optimizing grapevine water-use efficiency and root exploration under the climate-change scenario.

This is an open access article under the terms of the [Creative Commons Attribution](https://creativecommons.org/licenses/by/4.0/) License, which permits use, distribution and reproduction in any medium, provided the original work is properly cited.

© 2023 The Authors. *Physiologia Plantarum* published by John Wiley & Sons Ltd on behalf of Scandinavian Plant Physiology Society.

1 | INTRODUCTION

Transpirational water loss through stomata is often thought to be the wasteful result of photosynthetic CO₂ uptake (Cramer et al., 2009; Flexas, 2016). As such, classical eco-physiology often provides a plot in which photosynthesis (*A*) incurs a water cost and, over a period of time (e.g., minutes, days, and weeks), plants optimize intrinsic water-use efficiency (*WUE*) by adjusting *A* over stomatal conductance (*g_s*) fluctuations (Gago et al., 2014). Indeed, a tight, although nonlinear, relationship under steady-state conditions has often been observed between *g_s* and *A* (Faralli & Lawson, 2020) with asynchronous coordination under fluctuating natural conditions (Faralli, Bontempo, et al., 2022). Nevertheless, the absence of water-impermeable barriers at the stoma site may naively suggest other critical physiological functions of transpiration.

The conversion of water into water vapor during transpiration is vital for evaporative cooling under increasing air temperature and maintaining optimal leaf temperature for photosynthesis (Costa et al., 2012; Faralli, Bontempo, et al., 2022; Faralli, Pilati, et al., 2022; Frioni et al., 2019). Controversial, yet widely distributed plant behaviors (e.g., stomatal closure under high radiative and temperature conditions as well as nighttime transpiration; Coupel-Ledru et al., 2016) may not fully support the evaporative cooling principle and have been explained mainly by (1) embolism avoidance and (2) turgor maintenance/metabolites allocation, respectively (Hochberg et al., 2013). Some studies (Faralli, Bontempo, et al., 2022) suggest that dynamic responses to vapor pressure deficit (VPD) may partially account for contrasting observations to mid-day stomatal closure, although the function of nighttime water loss remains enigmatic (Fricke, 2019). Other studies provide evidence of the central role of the transpirational stream in mineral allocation within the plant (Polley et al., 1999; Pons & Bergkotte, 1996). However, *Arabidopsis* mutants with reduced stomatal density and hence *g_s* per unit of leaf area, do not show impaired nutrient uptake capacity (Hepworth et al., 2015), suggesting that transpiration is uncoupled from nutrient fluxes (Schulze & Bloom, 1984). This conclusion is partially confirmed by the observation in which the rate of transpiration, for example, in *Helianthus annuus* (Tanner & Beever, 2001), exceeds the rate required for root-to-shoot solute transport. In essence, the hypothesis in which transpiration has multiple physiological meanings may be broader than generally ascribed.

A significant number of studies provide strong evidence of a link, often described as biphasic, between the transpiration rate and soil/leaf nutrient availability (Cramer et al., 2009; Matimati et al., 2014). It has been shown that transpiration can serve as a direct mineral acquisition process mainly because it can increase the water and nutrient movements to the roots following mass-flow (Cramer et al., 2009 and references therein). For instance, isohydric pines close their stomata at relatively high soil and plant water potentials and thus cannot maintain adequate transpiration and nutrient uptake during prolonged drought periods. These mechanisms can lead to severe nutrient imbalance that speeds up the onset of hydraulic failure and phloem dysfunction (Salazar-Tortosa et al., 2018). Indeed, interception of nutrients by roots depends on root proliferation (Kage, 1997), but

generally accounts for a small proportion of nutrient acquisition. In addition, lateral root growth and the production of new fine roots are also important acquisition strategies in several tree species (Cochetel et al., 2019). However, a large proportion of nutrient acquisition is carried out by water mass-flow through transpiration that results in a substantial delivery of nutrients to the root surface (Cramer et al., 2008). Mass flow and diffusion of nutrients are followed by the uptake into the root tissue and transport across a plasmalemma by specific transport systems for a given nutrient (e.g., the H⁺ symporters responsible for NO₃⁻ uptake [Verdenal et al., 2021]). However, for many nutrients, including nitrogen, mobility in the soil limits the uptake by the root rather than the activity of the plasmalemma transport systems (Kage, 1997). Taken together, the acquisition of nutrients via mass-flow may be one critical yet unexplored mechanism of transpiration control in several species.

Grapevine is the most important crop in the Mediterranean basin. There is longstanding evidence that grapevine transpiration can be determined by water availability (Clemens et al., 2022; Coupel-Ledru et al., 2016), total canopy area (Serra et al., 2014), and rootstock × scion interaction (Faralli et al., 2020; Serra et al., 2014). In our work, we additionally hypothesized that, assuming mass-flow as an important nutrient acquisition scheme, soil nitrogen availability should, at least partially, be involved in determining the transpiration rate per unit of leaf area. In addition, we hypothesized the existence of a series of mechanisms triggered by different levels of nutrient availability, such as enhanced root-shoot ratio, increased transpiration irrespective of root mass, or both, involved directly (stomatal opening) or indirectly (lack of xylem pH alkalization) to transpiration and stomatal control of water loss. Assuming that genetic gain for several adaptations to environmental stresses and/or soil types have been successful in grapevine rootstocks, phenotypic variation should be present for the above traits in hybrids selected for low mineral mobility (e.g., calcareous soil). In this work, we show the presence of a nitrate signal involved in the control of transpiration in grapevine potentially via modulation of root-driven mass-flow.

2 | MATERIALS AND METHODS

2.1 | Plant materials and experimental design

The experiments were carried out at the experimental sites of the Fondazione Edmund Mach (FEM, San Michele all'Adige, Italy, 46°11'26.8" N 11°08'08.1" E) either in a greenhouse or in a polytunnel. The material used was 2-year-old cuttings that were fully rehydrated for 1 week and then transplanted in soil to induce rooting. In Experiments 1 and 2, 1-year-old grapevine plants (Pinot noir grafted onto Kober 5BB) were transplanted in 1.5 L pots filled with the same amount (1000 g) of Ter-compost loam-based potting compost (Ter-compost). Plants were transplanted on 17 December 2021 and 10 March 2022 (Experiments 1 and 2, respectively) inside the FEM greenhouse with an average daily temperature of 25°C, relative humidity 70% and an average daily photosynthetic photon flux

density (PPFD) of $400 \text{ mmol m}^{-2} \text{ s}^{-1}$ from natural light supplemented with tungsten lamps (12/12 h light/dark photoperiod). The plants were pruned to one shoot and kept growing vertically via cane supports for 2 weeks while manually watered every 2 days to avoid developing soil moisture deficit. In Experiment 3, 1-year-old grapevine plants (Pinot noir grafted onto Kober 5BB) were transplanted in 40-L rectangular pots filled with a 45:45:10 mix of acid peat, sand, and Ter-compost substrate (as above) on 4 April 2022. Two plants per pot were planted on one side, and a fine plastic mesh was applied in the middle of the container to avoid root proliferation to the opposite side (i.e., forcing nitrogen acquisition via mass-flow). Plants were moved inside a polytunnel under natural light and pruned to one shoot. Watering was applied every 2 days to maintain adequate soil moisture. In Experiment 4, 1-year-old grapevine plants (Pinot gris grafted onto Paulsen 1103 and Fercal) were transplanted in 9-L pots filled with the same amount (3000 g) of Ter-compost loam-based potting compost (Ter-compost) and pH was manipulated for one treatment via application of calcium hydroxide (section below). Paulsen 1103 (*Vitis berlandieri* × *Vitis rupestris*) is widely used in European viticulture and known as a vigorous rootstock, while Fercal (31 Richter × Blanchard 1B) is well-known for its tolerance to limestone-induced chlorosis (Laucou et al., 2008). Plants were transplanted in June 2021, moved inside a polytunnel under natural light and growing conditions and pruned to one shoot. Experiment 1 consisted of a 2×2 factorial design ($n = 6$) aiming at reducing nitrogen availability in the soil with two levels of soil nitrogen (NO_3^- applied via a solution [$+\text{NO}_3^-$] and water [$-\text{NO}_3^-$]) and two levels of calcium hydroxide application (either water [$-C$] or calcium hydroxide [$+C$] yielding a soil pH of 6 and 9, respectively). Experiment 2 had five treatments ($n = 6$), a control (no nitrogen applied [$-N$]), one nitrate application only ($+\text{NO}_3^-$), a weekly nitrate application during growth ($+\text{NO}_3^-$ week), one ammonium application only ($+\text{NH}_4^+$), a weekly ammonium application during growth ($+\text{NH}_4^+$ week). Experiment 3 had two treatments ($n = 8$), nitrate applied next to the plant (5 cm distance from the shoot, acquisition via interception, INT) and nitrate applied 30 cm from the base of the plant and on the other side of a permeable mesh (acquisition via mass-flow, MS). Experiment 4 had a factorial 2×4 design ($n = 6-8$) with two levels of soil pH (control, pH 6 and alkaline, pH 9) and two levels of rootstock (Paulsen 1103, and Fercal). The dose application for each specific treatment in every experiment is described below. The environmental data at which the experiments were carried out are shown in Figure S1.

2.2 | Treatments application

In Experiment 1, treatments were applied weekly via ad hoc solutions (500 mL per pot) starting from 13 January 2021 (day after treatment [DAT] 0). Calcium hydroxide was applied in solution with water (1.5 g to 3 L, pH 11) weekly, while NO_3^- was applied as 3 g per pot of ammonium nitrate in solution with water (3 L). The same amount of water (i.e., 500 mL) was applied to the pots with no treatment requirement (i.e., $-\text{NO}_3^-$ and $-C$ combination). In Experiment 2, either ammonium nitrate or ammonium sulfate were applied (weekly or at the beginning

of the experiment, depending on the treatment) in a solution with water (250 mL) at 3 g per pot. The same amount of water (i.e., 250 mL) was applied to the pots with no treatment requirement (i.e., N). In Experiment 3, 8 g of ammonium nitrate was applied for each plant (16 g per container at 20 cm depth) by localizing the application either next to the plant (interception) or at 30 cm from the plant so that roots were unable to directly intercept the nitrogen source yet forced to acquire NO_3^- via mass-flow. In Experiment 4, 5 g of ammonium nitrate was applied per pot at the beginning of the experiment. The substrate had a 5.5 pH, and calcium hydroxide was used to correct pH to 9.5 in pH 9 treatments.

2.3 | In vivo assessment of gas exchange, chlorophyll fluorescence, and stomatal conductance

Unless specified, all measurements were carried out in the morning (8:00–11:00). In Experiments 1, 2, and 3, stomatal conductance (g_s) and quantum yield of photosystem II under light-adapted conditions (F_q'/F_m') was assessed via a Li-600 porometer (Licor, Lincoln, NE) ($n = 6-30$). Analyses were carried out on different days after the start of the experiment, under natural light conditions and in fully expanded leaves tagged for each plant to avoid confounding effects from leaf expansion and leaf age. In Experiment 3, nighttime g_s was assessed predawn (4:00–6:00), and the dynamic of daytime g_s was evaluated in the morning (7:00–12:00). In Experiment 4, analysis of g_s was carried out with an SC-1 Leaf Porometer (Decagon, Pullman, WA). Gas-exchange analysis was performed in Experiment 3 and on the same leaves used for porometer analysis with a Li-cor 6800 (Licor) ($n = 6-7$). The leaf cuvette was maintained at $400 \mu\text{mol mol}^{-1} \text{ CO}_2$ concentration (C_a), a leaf temperature of 29–30°C, PPFD of $1500 \mu\text{mol m}^{-2} \text{ s}^{-1}$. Air VPD was maintained at around 1.5 kPa for the first set of measurements, while it was increased at 3.5 kPa for the second set of measurements. Leaves were first equilibrated to the cuvette conditions until both CO_2 assimilation rate per unit of leaf area (A) and g_s reached steady state. Intrinsic water use efficiency ($iWUE$) was calculated as A/g_s . Dark respiration (R_d) was assessed by switching off the light unit and waiting until stabilization (5–10 min for each replicate).

2.4 | Leaf water potential analysis

Leaf water potential (LWP, midday, $n = 4-6$) analysis was carried out in Experiments 1 and 4 between 10:00 and 12:00. Briefly, fully expanded and light-exposed leaves were sampled and placed into a plastic bag and positioned inside a Scholander pressure chamber (Model 3000 Scholander Plant Water Status Console, ICT International). Readings of LWP were taken and expressed as MPa.

2.5 | Gravimetric analysis of plant water use

In Experiment 4, pot weighing and watering was carried out every morning between 7:00 and 8:00, and for each pot ($n = 7-9$) using a

balance (Ohaus defender 3000). Daily water use was calculated as $WU \text{ (mL)} = \text{pot weight DATn} - \text{pot weight DATn1}$.

2.6 | Xylem sap pH

In Experiment 1, fully expanded leaves were used for sap extraction. Before sap extraction, the pressure chamber was fixed at a specific angle, facilitating the formation of almost uniform drops and the collection of the exudates in 1.5 mL Eppendorf vials that fit onto the petiole. Overpressure was applied at a constant rate until the applied pressure reached 1 MPa, at which point the first drop was collected. Then two additional pressures were applied, corresponding to 2 and 2.5 MPa, respectively. The amount of sap collected was approximately 600–700 μL . The pH values of the exudates from each fraction were immediately measured using a portable pH meter (Pal-pH). Xylem sap pH values were measured in $n = 4$ –6 leaves obtained from six different plants per treatment.

2.7 | Mineral content of leaves

Leaves used for g_s analysis were sampled in Experiments 1 and 4 ($n = 4$ –6). All samples were washed, oven-dried (80°C for 24 h), ground, and analyzed for total nitrogen (N), phosphorus (P), and potassium (K) composition. N was determined by the Dumas total combustion method with an elemental analyzer CN (Primacs SNC-100, Skalar Analytical), and the other elements concentration by Inductively Coupled Plasma-Optical Emission Spectrometry Spectroscopy plasma emission (ICP-OES) (Optima8300, PerkinElmer®, MA) spectroscopy following acid digestion with concentrated nitric acid (100°C for 2 h). For acid digestion of samples by a microwave oven (UltraWAVE, Milestone), an aliquot of about 300 mg of leaves was weighed into a polytetrafluoroethylene tube (UltraWAVE, Milestone) and 4 mL of HNO_3 was added. Accuracy was assured by analyzing a certified reference material at the start and the end of each analytical batch (NIST 1572 “citrus leaves,” National Institute of Standards and Technology). An online internal standard solution of Y at 1 mg L^{-1} was used during the analysis. Moreover, the use of argon as an online internal standard minimized eventual signal drift in ICP-OES analysis. The detection limit (DL) of each element was calculated as 3 times the standard deviation of the signal of the blank sample, analyzed 10 times (0.01 g kg^{-1} for both P and K). The quantification limits were estimated as 0.1%, 0.02%, and 0.15% for N, P, and K, respectively.

2.8 | Stable isotope analysis

Carbon and oxygen isotopic composition analysis was carried out in Experiments 1 and 4. Mature leaves used for g_s analysis were collected and placed immediately in an oven at 80°C for 48 h to allow complete dehydration. $\delta^{13}\text{C}$ was analyzed in 2 mg aliquots of leaf samples weighed in tin capsules, $\delta^{18}\text{O}$ in 0.2 mg aliquots weighed in silver capsules. Samples were combusted using a Vario Isotope Cube

Elementar Analyser (Elementar Analysensysteme GmbH), and the resulting CO_2 and N_2 gases were transferred to an isotope ratio mass spectrometer (Vislon, Elementar Analysensysteme GmbH) via a continuous flow-through inlet system. Samples were measured in triplicate. $\delta^{18}\text{O}$ was measured using an isotope ratio mass spectrometer (Finnigan DELTA XP, Thermo Scientific) after complete pyrolysis in an elemental analyzer (Finnigan DELTA TC/EA, high-temperature conversion elemental analyzer, Thermo Scientific). Samples for $\delta^{18}\text{O}$ were analyzed in duplicate. The isotope ratios were expressed in δ against V-PDB (Vienna-Pee Dee Belemnite) for $\delta^{13}\text{C}$ and V-SMOW (Vienna-Standard Mean Ocean Water) for $\delta^{18}\text{O}$ according to the following equation:

$$\delta i E = (i \text{ RSA} - i \text{ RREF}) / i \text{ RREF},$$

where RSA is the isotope ratio measured for the sample and RREF is the international standard isotope ratio. Delta values are multiplied by 1000 and commonly expressed in units (‰) (Coplen, 2011). The isotopic values for $\delta^{13}\text{C}$ and $\delta^{15}\text{N}$ were calculated through the development of a linear equation against working in-house standards, which were themselves calibrated against international reference materials: potassium nitrate IAEA-NO3 (IAEA-International Atomic Energy Agency) for $^{15}\text{N}/^{14}\text{N}$, L-glutamic acid USGS 40 (U.S. Geological Survey, Reston, VA) for $^{13}\text{C}/^{12}\text{C}$ and $^{15}\text{N}/^{14}\text{N}$, fuel oil NBS-22 and IAEA-CH-6 for $^{13}\text{C}/^{12}\text{C}$, Canadian Lodgepole pine USGS54 and South African red ivory wood USGS56 for $^{18}\text{O}/^{16}\text{O}$. For $\delta^{13}\text{C}$ and $\delta^{18}\text{O}$, the uncertainty of measurement (calculated as one standard deviation) was 0.1‰ and 0.3‰, respectively. Each reference material was measured in duplicate at the start and end of each daily group of sample analyses (each sample was also analyzed in duplicate). Control material was also included in the analyses of each group of samples to check the measurement's validity. The accepted maximum standard deviations of repeatability were 0.3‰ for $\delta(^{13}\text{C})$ and 0.5‰ for $\delta(^{18}\text{O})$.

2.9 | Root aquaporins gene expression analysis by RT-qPCR

In Experiment 3, fine roots (<3 mm diameter) were collected at the end of the experiment (see the section below) from INT and MS plants and immediately frozen with liquid nitrogen and kept at -80°C . For total RNA isolation, about 0.5 g of root material ($n = 3$) was grinded to a fine powder, and RNA was extracted using the Plant Total RNA Kit (Sigma-Aldrich) following the manufacturer's protocol. RNA quality was checked on agarose gel and by measuring the absorbance ratios 260/230 and 260/280. Possible genomic DNA contaminations were removed by DNase treatment using the TURBO DNA-free™ Kit (Thermo Fisher). Reverse transcription and quantitative PCR were performed in a single reaction system using the SuperScript® III Platinum® SYBR® Green One-Step qRT-PCR kit (Thermo Fisher) and a ViiA7 thermocycler (Applied Biosystems, Waltham, MA) in a total reaction volume of 10 μL . Briefly, each reaction contained: 0.2 μL of SuperScript® III RT/Platinum® Taq Mix (includes RNaseOUT™), 5 μL of 2X SYBR® Green Reaction Mix, 0.2 μL of 10 μM of forward primer

and reverse primer, 0.02 μL of ROX Reference Dye, 3.38 μL of DEPC-treated water, 1 μL of total RNA. Thermal cycling conditions were as follows: 50°C for 3 min, 95°C for 5 min, then 40 cycles of 95°C for 15 s, 60°C for 30 s, followed by a single step of 60 s at 40°C. To ensure single-product amplification, melting curve analysis was performed. Gene specific primers were designed with Primer 3 web service version 4.1.0 (<https://primer3.ut.ee/>) with default parameters on the Kober 5BB putative orthologues of three *Vitis vinifera* aquaporin PIP genes (VvPIP1;1, VvPIP2;1, and VvPIP2;2) (Vandeleur et al., 2014). The three Kober 5BB putative PIP genes were identified by sequence similarity search on the Kober 5BB diploid genome assembly available on the website <http://www.grapegenomics.com> using the *Vitis vinifera* sequences as query. VvActin-7 (AM465189.1) was used as a reference gene as it was previously proposed for aquaporin analysis in grapevine by Vandeleur et al. (2009). The primers' sequence and the corresponding *Vitis vinifera* and Kober 5BB reference genes are reported in Table S1. Relative expression of the three PIP genes in the root was calculated with the comparative Ct method (Schmittgen & Livak, 2008). Data are reported as fold change of the expression in the treated samples compared to the control ones (calibrator).

2.10 | Morphological assessment of plant biomass

At harvest (11 March 2022 for Experiment 1, 04 July 2022 for Experiment 3, and 03 September 2021 for Experiment 4), the above-ground biomass of each vine was harvested ($n = 6-9$). The material was then dried for 48 h at 80°C and weighed (Ohaus defender 3000) to get the total biomass dry weight (DW, g). Roots were carefully washed, dried, and weighed. Root:shoot ratio was then calculated as the ratio between above and below-ground dry weight. In Experiment 1, specific leaf area (SLA) was calculated for fully expanded leaves ($n = 6$) as the ratio between leaf area estimated via ImageJ and the dry weight after 48 h at 80°C.

2.11 | Statistical analysis

All the analyses were carried out with Rstudio (R Core Team 2018) by using either the *stats*, *agricolae*, or *ggplot2* packages. All traits were subjected to two-way ANOVA and one-way ANOVA depending on factor number. Association between traits was assessed via linear or segmented regression. All data were checked for normality and equality of variance through visual assessment of distribution and residuals versus fitted values. Means separation ($p < 0.05$) was carried out via Tukey's test.

3 | RESULTS

3.1 | Stomatal conductance, gas-exchange, water-use, and leaf water status at different levels of nutrient availability

In Experiment 1, data collected on different days from treatment application revealed a general trend in which progressive limitation in

NO_3^- increased g_s in grapevine leaves. The increase in g_s was more pronounced for DAT 32 (Figure 1A), while the effect was lower (although still significant [$p < 0.001$]) for the last experimental period (DAT 39–40). However, the increase in g_s was evident only for data collected in the early morning with a VPD of around 1–1.5 kPa as increases in VPD (2–3 kPa) reduced g_s for $-\text{NO}_3^-$ plants to similar levels to $+\text{NO}_3^-$ plants (Figure 1B). LWP of $+\text{NO}_3^-$ leaves was significantly ($p = 0.014$) less negative than $-\text{NO}_3^-$ plants, while no effects were observed for C treatments. Alkalinization of xylem sap was evident for NO_3^- plants subjected to $+\text{NO}_3^-$ –C treatments, while minimal effects were observed for the other treatments (Figure 1D). No significant effects or interactions with NO_3^- were observed when C was applied.

In Experiment 3, vines intercepting the nitrogen source (INT) had lower g_s than the plants forced to acquire nitrogen via mass-flow (MS) in DAT 15 ($p < 0.001$), while in DAT 4 no significant differences were observed ($p = 0.174$; Figure 2A,B). No differences between treatments were observed for predawn g_s , while the differences were overall significant at DAT 20 throughout the early morning ($p < 0.001$) when PPFD was not saturating and VPD below 1.5 kPa (Figure 2C). Gas-exchange measurements highlighted no differences for A between treatments ($p = 0.0949$ and $p = 0.392$ at VPD leaf of 1.50 and 2.91, respectively), while g_s was higher in MS plants when compared to INT plants when VPD was not limiting (Figure 2D,E). On the contrary, no differences in g_s were observed between treatments at high VPD (Figure 2E). Overall, $w\text{WUE}$ was increased at high VPD and was higher in INT plants at low VPD ($p = 0.004$) compared to MS plants, although no significant differences were observed at high VPD (Figure 2E).

Under developing soil nutrient limitation induced by soil pH modulation, significant effects were observed for daily water use when different rootstocks were tested (Figure 3A,B). Although a trend was observed in increasing water-use in 1103 Paulsen, WU was reduced from DAT 18 ($p < 0.05$) in vines subjected to alkaline soil. On the contrary, Fercal subjected to high soil pH maintained a higher WU when compared to pH 6 throughout the experimental period, although differences were observed between days. The data are partially confirmed by g_s analysis at DAT 16 in which a significant increase in g_s ($p = 0.010$) was recorded under pH 9 (Figure 3B). The increase in g_s at pH 9 was not present in 1103 Paulsen. The response of WU to average daily VPD shows a similar breakpoint (BP) of transpiration for all rootstocks and soil pH, although the slope of the linear segment was higher in Fercal under pH 9 (Figure 3C). Chlorophyll content analysis provides evidence of a general negative effect of alkaline soil on leaf chlorophyll a and b ($p < 0.05$; Figure 3D). However, the reduction in leaf chlorophyll a and b was overall more pronounced in 1103 Paulsen than Fercal when subjected to soil pH 9 compared to pH 6.

3.2 | Foliar nutrients and stable isotopes at different levels of nutrient availability

Foliar [N] was significantly reduced at the time of harvest (DAT40) in Experiment 1 (Figure 4A) when no NO_3^- was applied. No

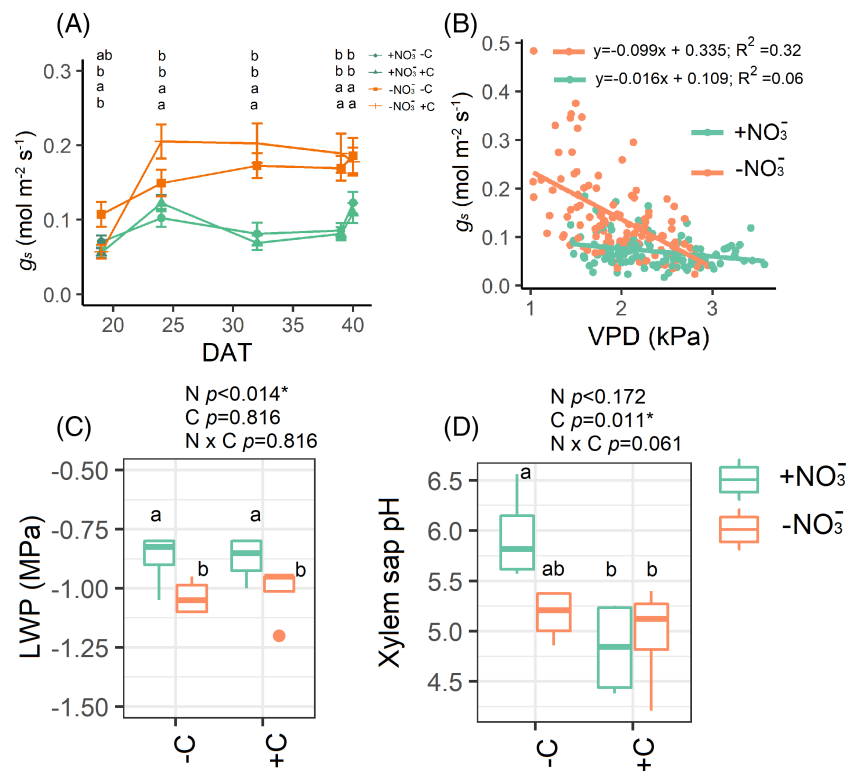


FIGURE 1 The dynamic of leaf stomatal conductance (g_s) in vines subjected to two levels of soil nitrogen (NO_3^- applied via a solution [$+\text{NO}_3^-$] and water [$-\text{NO}_3^-$]) and two levels of calcium hydroxide application (either water [$-\text{C}$] or calcium hydroxide [$+\text{C}$]) (A). Data were collected in vivo with a Li-cor 600 and under ambient temperature and light conditions on days after treatment application (DAT) 19, 24, 32, 39, and 40 (A) ($n = 10\text{--}45$). Data are means, error bars represent the standard error of the mean (SEM), while different letters represent significant differences between treatments according to Tukey's test. (B) Relationship between g_s and vapor pressure deficit (VPD), points are raw data and fitted with linear regression. (C) Leaf water potential ($n = 4$) for the same treatments is shown, while in (D) xylem sap alkalization is presented ($n = 4$). In graphs, points represent raw data, horizontal lines within boxes indicate the median and boxes indicate the upper (75%) and lower (25%) quartiles. Whiskers indicate the ranges of the minimum and maximum values. Data were analyzed with two-way ANOVA and p -values are shown in the graph, while different letters represent significant differences between treatments according to Tukey's test. Data are from Experiment 1.

significant effect was observed for [N] and soil alkalization ($\pm \text{C}$). On the contrary, soil [P] was mainly affected and reduced by C ($p < 0.001$), and a borderline effect at increasing foliar [K] ($p = 0.055$) was observed for C (Figure 4B,C). The general very negative $\delta^{13}\text{C}$ values also indicated no water stress in these plants, as may be expected since the soil was kept close to field capacity. Carbon isotope composition was significantly lower for plants that received no NO_3^- ($p < 0.001$) while C did not have a significant effect (Figure 4D). A significant negative correlation (Figure 4E, $p < 0.001$) was observed between g_s (DAT40) and foliar [N]. Similarly, a strong correlation was observed between $\delta^{13}\text{C}$ and N:P ratio (Figure 4F, $p < 0.001$) as a proxy of excess in [N].

Foliar [N], [P], and [K] were not affected when vines were forced to acquire minerals via mass-flow (Figure 5A-C). Similarly, the N:P ratio was unaffected ($p = 0.863$). Analysis of $\delta^{13}\text{C}$ did not provide significant differences between treatments, while significant differences were observed for $\delta^{18}\text{O}$ with INT associated with higher $\delta^{18}\text{O}$ when compared to MS plants ($p = 0.007$, Figure 5E,F).

3.3 | Root aquaporins expression under forced mass-flow acquisition

In Experiment 3, no significant changes were observed in the expression level of root *PIP2.1* and *PIP2.2* in MS plants compared to INT vines (Figure 6B,C, $p > 0.05$). On the contrary, a significant increase in *PIP1.1* expression level was observed for vines forced to acquire nitrogen via mass-flow (MS) when compared to vines intercepting the nitrogen source (INT; Figure 6A, $p = 0.022$).

3.4 | Shoot and root biomass at different levels of nutrient availability

Shoot biomass in Experiment 1 showed significant variation between treatments, with N being the main factor affecting above-ground dry weight ($p < 0.001$; Figure 7A). Similarly, in Experiment 4, soil pH reduced shoot dry weight by 35% in 1103 Paulsen, while no significant differences were observed in Fercal. Forcing mass flow

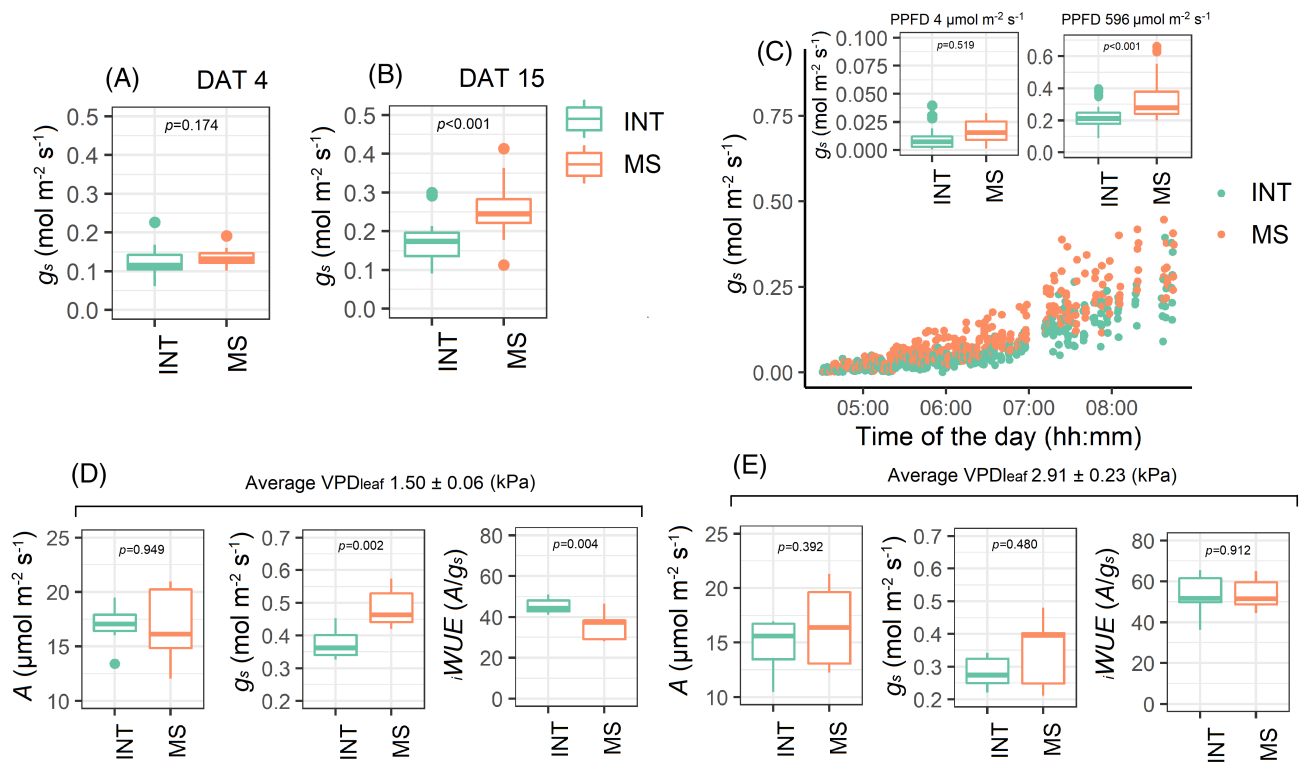


FIGURE 2 (A,B) Dynamic of leaf stomatal conductance (g_s) in vines intercepting the nitrogen source (INT) or forced to acquired nitrogen via mass flow (MS) in DAT 4 and DAT 15. Data were collected in vivo with a Li-cor 600 and under ambient temperature and light conditions ($n = 8-32$). In C, the dynamic of g_s was monitored pre- and postdawn (points are raw data) and g_s at specific PPFD values (nighttime and sub-saturating PPFD) are shown ($n = 24-36$). In D and E, gas exchange data (A — CO_2 assimilation rate per unit of leaf area, g_s —stomatal conductance, and $iWUE$ — A/g_s ratio) were collected at saturating light and two contrasting VPD levels (1.50 and 2.91 kPa on average) ($n = 8$). In graphs, points represent raw data, horizontal lines within boxes indicate the median and boxes indicate the upper (75%) and lower (25%) quartiles. Whiskers indicate the ranges of the minimum and maximum values. Data were analyzed with one-way ANOVA and p -values are shown in the graph. Data are from Experiment 3.

acquisition of nitrogen in Experiment 3 (MS) did not reduce biomass ($p = 0.805$). Root biomass was progressively increased at increasing nutrient limitation in Experiment 1 (Figure 7A, N $p < 0.001$, C $p = 0.010$), while in Experiments 3 and 4 (Figure 7B–C), root biomass was unaffected by the treatments. However, a trend for the $R \times P$ interaction was observed as Fercal significantly increased roots DW at pH 9 compared to pH 6. The root-to-shoot ratio was therefore increased under nutrient limitation ($-\text{NO}_3^-$, +C, or pH 9, $p < 0.001$) in Experiments 1 and 4, while no significant differences were observed for Experiment 3.

4 | DISCUSSION

4.1 | Stomatal functionality is tightly linked with mineral acquisition via mass-flow in grapevine

It has been shown that stomatal regulation in grapevine is determined by numerous and interdependent signals with biochemistry (hormonal) and hydraulics governing the interplay between transpiration and evaporative demand, soil water status, light, and air

temperature (Gambetta et al., 2020; Tombesi et al., 2015). However, only a few reports focused on the relationship between stomatal control of transpiration and nutrient availability in grapevine. In a 2-year field trial, Taskos et al. (2020) showed more negative $\delta^{13}\text{C}$ in leaves of non-N-fertilized Cabernet Sauvignon, while less negative values were observed at increasing nitrogen supply, suggesting increased $iWUE$ at increasing N input. Indeed, the relationships between leaf [N] and g_s highlighted the presence of a biphasic response in which g_s was strongly reduced at low [N] (below 1.5%) and, although to a lesser extent, at [N] above 3%. This study is in line with the data from Experiment 1, in which higher $iWUE$ via low g_s and less negative $\delta^{13}\text{C}$ were observed in leaves with [N] close to 30 mg g^{-1} . In addition, in Experiment 3, gas-exchange analysis showed no significant effects of NO_3^- distancing on A , suggesting g_s as a primary modulator of water-use efficiency. Indeed, Cramer et al. (2009) proposed three nonmutually exclusive ways of mineral regulation of transpiration: (1) upregulation of aquaporins that led to an increased hydraulic conductance of the roots, (2) g_s stimulation via NO production, and (3) lack of apoplastic pH alkalization and hence g_s maintenance via lower stomatal sensitivity to ABA. We provided evidence that, under optimal environmental conditions (low VPD,

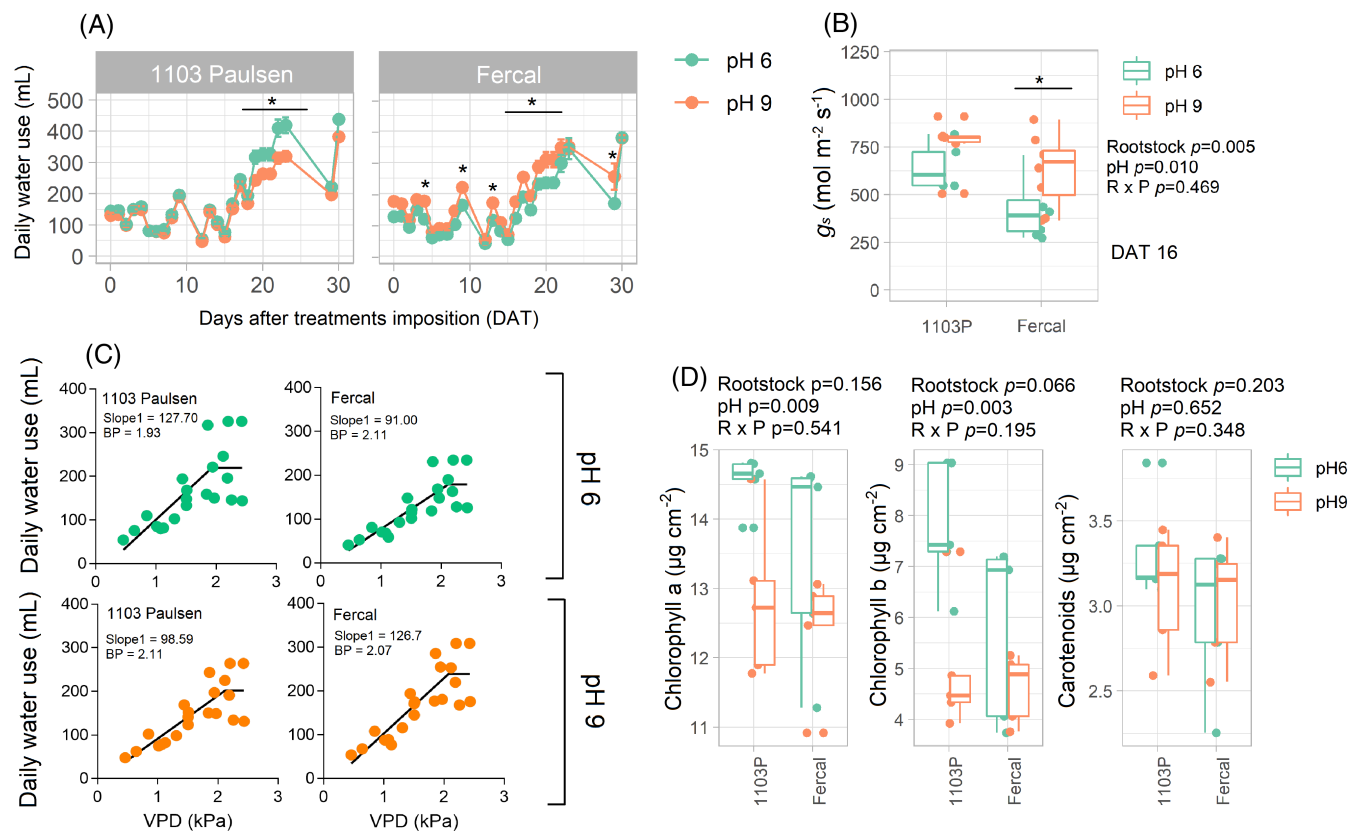


FIGURE 3 (A) Dynamic of daily water-use for Pinot gris grafted into 1103 Paulsen and Fercal and grown in control soil (pH 6) and alkaline soil (pH 9). Points are means ($n = 6-9$) and error bars represent standard error of the mean (SEM). Asterisks represent significant differences between soil treatments according to one-way ANOVA ($p < 0.05$). In B, stomatal conductance (g_s) for Pinot gris grafted into 1103 Paulsen and Fercal and grown in control soil (pH 6) and alkaline soil (pH 9) ($n = 10$) collected in DAT 16. In the graph, points represent raw data, horizontal lines within boxes indicate the median and boxes indicate the upper (75%) and lower (25%) quartiles. Whiskers indicate the ranges of the minimum and maximum values. Data were analyzed with one-way ANOVA and p -values are shown in the graph. In C, daily water-use as a function of average daily VPD. Data are means ($n = 6-9$) and fitted via a piecewise function. Output of slope for the first linear segment and breakpoint (BP) are shown in the graph. In D, leaf chlorophyll a , b , and carotenoids are shown. In the graph, points represent raw data, horizontal lines within boxes indicate the median, and boxes indicate the upper (75%) and lower (25%) quartiles. Whiskers indicate the ranges of the minimum and maximum values. Data were analyzed with one-way ANOVA ($n = 6$) and p -values are shown in the graph. Data are from Experiment 4.

ideal water status), plant water-use and g_s were higher in vines in which nitrogen was near-limiting (high pH, low N availability) or only accessible via mass-flow. This was both associated with a reduction in xylem sap alkalization (Experiment 1) and overexpression of root aquaporins (i.e., PIP1.1, Experiment 3), suggesting that the proposed mechanisms by Cramer et al. (2009) may not be mutually exclusive, at least for the genetic material used in this work. In addition, significant differences in g_s between nitrate and ammonium application were observed (as already proposed by Cramer et al. [2009]), with the latter showing limited effect when compared to control untreated (Figure S2, Experiment 2). While in Experiments 1 and 4, the increase in R:S ratio may partially explain the differences in transpiration between treatments, the lack of significant morphological differences (shoot and roots) in Experiment 3 provided evidence of a physiological control of mass-flow, confirmed by the consistent differences in either $\delta^{13}\text{C}$ or $\delta^{18}\text{O}$. Further work should focus on understanding the physiological determinants associated with the nitrogen modulation of g_s in grapevine.

4.2 | Stress conditions hierarchically superimpose over nitrogen signals

In grapevine, a species with tight stomatal control (although genotypic variation has been shown to be present, for example, Dal Santo et al. (2016), Bertamini et al. (2021)) compared to other species (e.g., grasses) characterized by nonconservative behaviors (Faralli et al., 2019), hydraulic signals seems to play a critical role on stomatal closure with additional input from ABA under water stress, heat stress and elevated evaporative demand (Faralli, Bontempo, et al., 2022; Faralli, Pilati, et al., 2022; Tombesi et al., 2015). In our work and for all experiments, the nonconservative response found under low N input was nullified by the naturally occurring VPD dynamic during daytime. Gas-exchange analysis confirmed this trend, and in Experiment 3, the nonsignificant differences between treatments for $\delta^{13}\text{C}$ provide evidence of a loss of nonconservative behavior in MS plants under high evaporative demand. However, $\delta^{18}\text{O}$ data showed conserved higher g_s in MS plants in contrast to $\delta^{13}\text{C}$. INT could be more inclined to

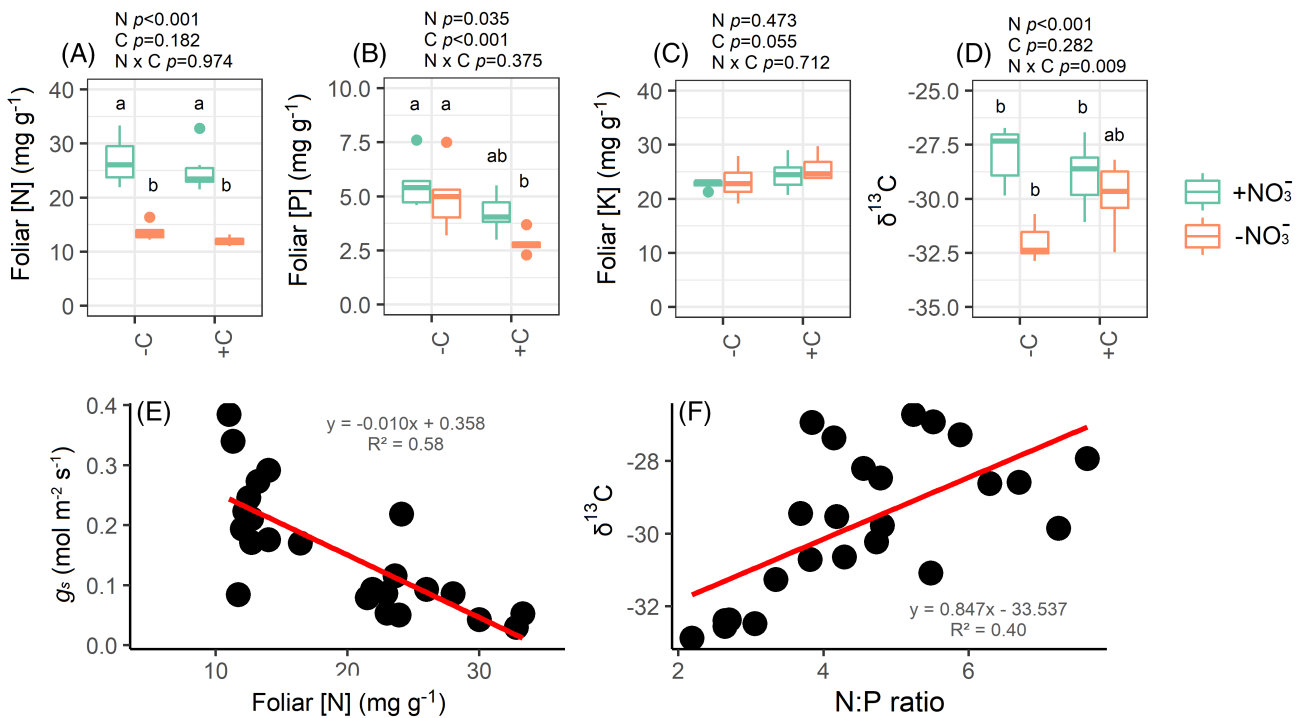


FIGURE 4 Foliar nitrogen concentration (A), foliar phosphorus concentration (B), foliar potassium concentration (C), and carbon isotopic composition (D) in vines subjected to two levels of soil nitrogen (NO₃⁻ applied via a solution [+NO₃⁻] and water [-NO₃⁻]) and two levels of calcium carbonate/calcium hydroxide application (either water [-C] or calcium carbonate/calcium hydroxide [+C]). Samples were collected in DAT40 for Experiment 1. In the graph, points represent raw data, horizontal lines within boxes indicate the median and boxes indicate the upper (75%) and lower (25%) quartiles. Whiskers indicate the ranges of the minimum and maximum values. Data were analyzed with two-way ANOVA and *p*-values are shown in the graph while different letters represent significant differences between treatments according to Tukey's test. In E and F, the relationship of foliar [N] with *g_s* and foliar N:P with δ¹³C is shown. The regression equation and coefficient of determination (R²) are shown in the graph where data points are raw data. Data are from Experiment 1.

photorespiration losses under hot conditions since a tighter stomatal regulation of transpiration can reduce evaporative leaf cooling aimed at increasing heat dissipation (e.g., Figure 1C). A higher vulnerability to leaf overheating, at least during the progressive natural increase in morning VPD (Figure 1C) in INT, would enhance respiratory losses ($p = 0.086$, Figure S3), reduce *A* and impede any decrease in substomatal CO₂ concentration despite a similar leaf [N] (Figure 5). Taken together, the data may suggest a complex interplay between N availability and distance application with potential signals nullified or reduced by environmental stresses. However, potential preferable effects from higher *g_s* following N fertilization distancing may be expected under hot conditions and should be tested in specific field trials.

4.3 | Does rootstock breeding for high soil pH has unintentionally selected for mass-flow acquisition?

Breeding for novel grapevine rootstocks was intensively carried out in the early 1900, and only a few new genotypes have been recently released (Ollat et al., 2014). Thus, it is conceivable that one of the major bottlenecks in rootstock breeding remains the lack of underlying physiological traits to focus on improvement. While in other

species, physiological breeding is ongoing and prosperous (Reynolds et al., 2009), in grapevine rootstock morphological traits (root depth, root angle, induced vigor, and grafting compatibility) governs breeding efforts also given the complex and heterogeneous pedo-climatic conditions in which grapevine is grown (i.e., lack of reproducibility) and owing to the still enigmatic yet widely reported bi-directional interactions between scion and rootstock (Clingeffer et al., 2019; Tandonnet et al., 2010). Our work morphologically confirms biomass maintenance in Fercal subjected to a high soil pH compared to 1103 Paulsen accompanied by higher leaf chlorophyll. Interestingly, these traits were associated with a high pH-induced increase in *g_s* for Fercal as well as plant water-use that can be interpreted as a specific strategy of the rootstock to enhance nutrient mass-flow thus boosting mineral acquisition capacity (e.g., Rosdeutsch et al., 2021; Zamboni et al., 2016). The increase in root mass under pH 9 in Fercal, when compared to 1103 Paulsen, also suggests preferable mechanisms that may be linked to an enhanced mineral uptake capacity and root exploration under moderate-to-high limiting conditions. We speculate that breeding for rootstocks tolerant to calcareous soils has unintentionally selected for material with enhanced mass-flow traits that can explore higher proportions of dissolved minerals in the rhizosphere. Bringing this evidence to the context of climate change and increase in atmospheric [CO₂] that

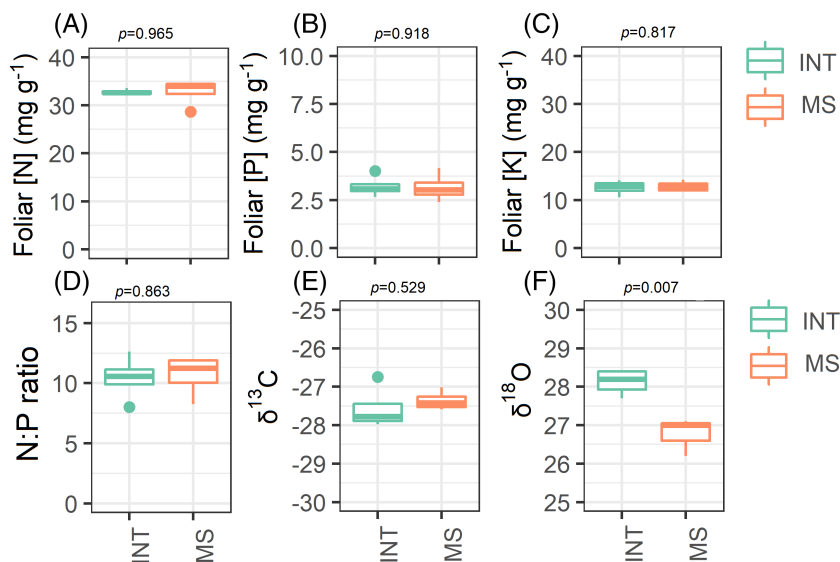


FIGURE 5 Foliar nitrogen concentration (A), foliar phosphorus concentration (B), foliar potassium concentration (C), N:P ratio (D), carbon isotopic composition (E) and oxygen isotope composition (F) in vines intercepting the nitrogen source (INT) or forced to acquire nitrogen via mass flow (MS). In the graph, points represent raw data, horizontal lines within boxes indicate the median and boxes indicate the upper (75%) and lower (25%) quartiles. Whiskers indicate the ranges of the minimum and maximum values. Data were analyzed with one-way ANOVA ($n = 3-4$) and p -values are shown in the graph.

have been recently highlighted as a primary factor in N deficiency in plants and photosynthetic acclimation (Gojon et al., 2022), enhancing mass-flow or selecting for the specific trait may be a major strategy to minimize the long-term negative effects of elevated [CO₂]. Although the trait can be surely utilized in grapevine rootstock improvement, this relatively conserved dynamic (e.g., Cramer et al., 2009) may guide breeding efforts under increasing [CO₂] in different agriculturally important crops.

4.4 | Manipulation of fertilization practices for contrasting water conservation strategies?

Fertilization practices in grapevine have been subjected to significant improvements. For instance, variable rate technologies are now considered critical to provide site- and plant-specific fertilization when combined with NDVI and vigor analysis, thus avoiding under- or over-fertilization (Gatti et al., 2020). However, to our knowledge, the possible interaction between mineral availability/application distance from the roots and the water-use dynamics has never been extensively explored. Only in a recent study, the potential exploitation of the root:shoot acclimation to N deficiency has been hypothesized as a potential signal for inducing root proliferation and hence ameliorated water extraction from the soil in grapevine (Dinu et al., 2022). We additionally propose nitrogen fertilizer (in this case, nitrate) as an important candidate for further exploiting mechanisms related to transpiration efficiency and hence stress tolerance in grapevine via three nonmutually exclusive approaches. First, a transient N limitation may induce an inflated root:shoot ratio providing higher root surface and water extraction in conditions of prominent soil depth. Secondly, forcing mass-flow acquisition may partially confer nonconservative responses, for example, in the morning when VPD is still optimal for photosynthesis and provide early stomatal opening and ideal leaf gas-exchange in the most valuable period of the day for carbon acquisition. This may be achieved by a specific approach of mineral fertilization distancing from

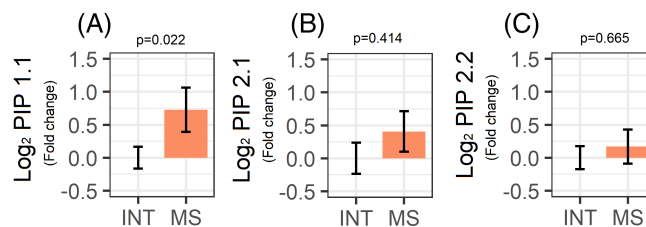
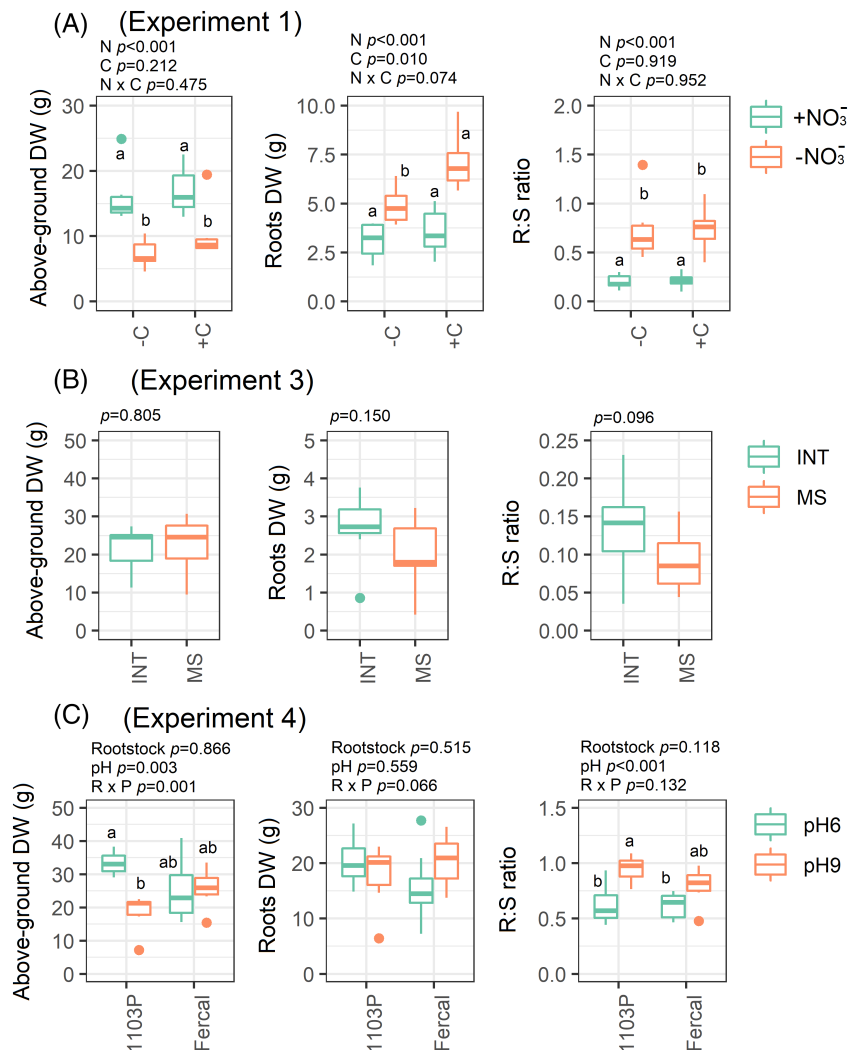


FIGURE 6 Relative gene expression of three PIP genes (PIP1.1 [A], PIP2.1 [B], and PIP2.2 [C]) in Kober 5BB roots (Experiment 3) of vines forced to acquire nitrogen via mass flow (MS) relative to vines intercepting the nitrogen source (INT). In the graph, data are means and error bars represent the standard error of the mean (SEM). Data were analyzed with one-way ANOVA ($n = 3$) and p -values are shown in the graph.

the plant that may increase losses via leaching but, at the same time, also avoid under-row competition for minerals between the vine and weeds. Finally, focusing on the reverse aspect of the grapevine water-use, reducing the fertilization distancing from the roots or even increasing N input may result in a significant tighter stomatal control of transpiration, leading to higher water-use efficiency and water conservation per unit of leaf area. Since this trend has probably been exacerbated in recent years by the increasing amount availability of fertilizers (i.e., a general trend in increasing μ WUE) or via foliar application of nitrogen-based biostimulants, (Gutiérrez-Gamboa et al., 2019) the critical trade-off between water conservation and evaporative cooling (i.e., saving water or dissipating heat?) in grapevine has been unintentionally weighed towards a tighter water conservation strategy. This, along with the partial stomatal closure observed under the occurring increase in atmospheric (CO₂; Stevens et al., 2021) has theoretically increased the susceptibility of the productive vineyards to heat stress. In essence, although further and extensive work is required in natural field conditions, we propose nitrogen fertilization as a potential candidate for fine-tuning strategies against abiotic stresses in grapevine.

FIGURE 7 Above-ground dry biomass, root dry biomass, and root-shoot ratio ($n = 4-9$) for Experiment 1 (A), Experiment 3 (B), and Experiment 4 (C). In the graph, points represent raw data, horizontal lines within boxes indicate the median and boxes indicate the upper (75%) and lower (25%) quartiles. Whiskers indicate the ranges of the minimum and maximum values. Data were analyzed with two-way ANOVA and p -values are shown in the graph while different letters represent significant differences between treatments according to Tukey's test for factorial experiments. Data are from Experiment 1 (A), 3 (B), and 4 (C).



5 | CONCLUSIONS

In our study, we provide evidence of the sensitivity of grapevine transpiration to soil nitrogen, suggesting the transpiration-derived mass-flow as an additional critical process associated with stomatal water loss. Reducing or distancing N increases g_s , although increasing VPD progressively dims the variability observed between treatments suggesting that grapevine prioritizes defensive mechanisms against abiotic stresses over mineral acquisition. These traits may be exploited in rootstock breeding or vineyard management, although further field studies are required to confirm the reproducibility of the responses in multiple environments and genetic material. Given the increasingly negative effects, that climate change is imposing on viticulture, taking advantage of unexploited signals, and novel traits may effectively define innovative and valuable strategies for viticulturists.

AUTHOR CONTRIBUTIONS

MF planned the experiments, conducted the work, interpreted and analysed the data and wrote the manuscript; PLB planned the experiments, conducted the work and reviewed the manuscript; CM carried out the gene expression analysis and reviewed the manuscript; LB

carried out the isotopic analysis and reviewed the manuscript; MB helped with data interpretation, supervised the studies and reviewed the manuscript; all co-authors reviewed the final draft.

ACKNOWLEDGMENTS

The authors would like to thank Guan Lubin, Daniela Bertoldi, Oscar Giovannini, Leonardo Negri, and Edoardo Salvetta for their help during different steps of data collection and analysis. We thank Alessia Fortunati from Ecossearch for the use of the Li-cor 6800. Open Access Funding provided by Università degli Studi di Trento within the CRUI-CARE Agreement.

CONFLICT OF INTEREST STATEMENT

The authors declare no conflict of interest.

DATA AVAILABILITY STATEMENT

The data that support the findings of this study are available from the corresponding author upon reasonable request.

ORCID

Michele Faralli  <https://orcid.org/0000-0002-7933-6142>

REFERENCES

- Bertamini, M., Faralli, M., Varotto, C., Grando, M.S. & Cappellin, L. (2021) Leaf monoterpene emission limits photosynthetic downregulation under heat stress in field-grown grapevine. *Plants*, 10(1), 181.
- Clemens, M., Faralli, M., Lagreze, J., Bontempo, L., Piazza, S., Varotto, C. et al. (2022) VvEPFL9-1 Knock-out via CRISPR/Cas9 reduces stomatal density in grapevine. *Frontiers in Plant Science*, 13, 878001.
- Clingeffer, P., Morales, N., Davis, H. & Smith, H. (2019) The significance of scion × rootstock interactions. *Oeno One*, 53(2), 335–346.
- Cochetel, N., Hévin, C., Vivin, P., Ollat, N. & Lauvergeat, V. (2019) Grapevine rootstocks differentially regulate root growth and architecture in response to nitrogen availability. *Acta Horticulturae*, 1248, 521–530. Available from: <https://doi.org/10.17660/ActaHortic.2019.1248.70>
- Coplen, T.B. (2011) Guidelines and recommended terms for expression of stable-isotope-ratio and gas-ratio measurement results. *Rapid Communications in Mass Spectrometry*, 25(17), 2538–2560.
- Costa, J.M., Ortuño, M.F., Lopes, C.M. & Chaves, M.M. (2012) Grapevine varieties exhibiting differences in stomatal response to water deficit. *Functional Plant Biology*, 39(3), 179–189.
- Coupeledru, A., Lebon, E., Christophe, A., Gallo, A., Gago, P., Pantin, F. et al. (2016) Reduced nighttime transpiration is a relevant breeding target for high water-use efficiency in grapevine. *Proceedings of the National Academy of Sciences*, 113(32), 8963–8968.
- Cramer, M.D., Hawkins, H.J. & Verboom, G.A. (2009) The importance of nutritional regulation of plant water flux. *Oecologia*, 161(1), 15–24.
- Cramer, M.D., Hoffmann, V. & Verboom, G.A. (2008) Nutrient availability moderates transpiration in *Ehrharta calycina*. *New Phytologist*, 179(4), 1048–1057.
- Dal Santo, S., Palliotti, A., Zenoni, S., Tornielli, G.B., Fasoli, M., Paci, P. et al. (2016) Distinct transcriptome responses to water limitation in isohydric and anisohydric grapevine cultivars. *BMC Genomics*, 17(1), 1–19.
- Dinu, D.G., Popescu, C.F., Sumedrea, D.I., Manolescu, A.E., Pandelea, L. M. & Rustioni, L. (2022) A new strategy to improve vineyard resilience: grapevine morphological adaptation to short-term nitrogen deficiency. *Agronomy*, 12(6), 1355.
- Faralli, M., Bianchedi, P.L., Bertamini, M. & Varotto, C. (2020) Rootstock genotypes shape the response of cv. Pinot gris to water deficit. *Agronomy*, 11(1), 75.
- Faralli, M., Bontempo, L., Bianchedi, P.L., Moser, C., Bertamini, M., Lawson, T. et al. (2022) Natural variation in stomatal dynamics drives divergence in heat stress tolerance and contributes to seasonal intrinsic water-use efficiency in *Vitis vinifera* (subsp. *sativa* and *sylvestris*). *Journal of Experimental Botany*, 73(10), 3238–3250.
- Faralli, M. & Lawson, T. (2020) Natural genetic variation in photosynthesis: an untapped resource to increase crop yield potential? *The Plant Journal*, 101(3), 518–528.
- Faralli, M., Pilati, S. & Bertamini, M. (2022) Post-veraison increase in source-sink ratio via manipulation of sink availability gradually reduces leaf functionality in grapevine (cv. Pinot noir). *Environmental and Experimental Botany*, 204, 105092.
- Faralli, M., Williams, K.S., Han, J., Corke, F.M., Doonan, J.H. & Kettlewell, P.S. (2019) Water-saving traits can protect wheat grain number under progressive soil drying at the meiotic stage: a phenotyping approach. *Journal of Plant Growth Regulation*, 38(4), 1562–1573.
- Flexas, J. (2016) Genetic improvement of leaf photosynthesis and intrinsic water use efficiency in C3 plants: why so much little success? *Plant Science*, 251, 155–161.
- Fricke, W. (2019) Night-time transpiration—favouring growth? *Trends in Plant Science*, 24(4), 311–317.
- Frioni, T., Saracino, S., Squeri, C., Tombesi, S., Palliotti, A., Sabbatini, P. et al. (2019) Understanding kaolin effects on grapevine leaf and whole-canopy physiology during water stress and re-watering. *Journal of Plant Physiology*, 242, 153020.
- Gago, J., Douthe, C., Florez-Sarasa, I., Escalona, J.M., Galmes, J., Fernie, A. R. et al. (2014) Opportunities for improving leaf water use efficiency under climate change conditions. *Plant Science*, 226, 108–119.
- Gambetta, G.A., Herrera, J.C., Dayer, S., Feng, Q., Hochberg, U. & Castellarin, S.D. (2020) The physiology of drought stress in grapevine: towards an integrative definition of drought tolerance. *Journal of Experimental Botany*, 71(16), 4658–4676.
- Gatti, M., Schippa, M., Garavani, A., Squeri, C., Frioni, T., Dosso, P. et al. (2020) High potential of variable rate fertilization combined with a controlled released nitrogen form at affecting cv. Barbera vines behavior. *European Journal of Agronomy*, 112, 125949.
- Gojon, A., Cassan, O., Bach, L., Lejay, L. & Martin, A. (2023) The decline of plant mineral nutrition under rising CO₂: physiological and molecular aspects of a bad deal. *Trends in Plant Science*, 28(2), 185–198.
- Gutiérrez-Gamboa, G., Romanazzi, G., Garde-Cerdán, T. & Pérez-Álvarez, E.P. (2019) A review of the use of biostimulants in the vineyard for improved grape and wine quality: effects on prevention of grapevine diseases. *Journal of the Science of Food and Agriculture*, 99(3), 1001–1009.
- Hepworth, C., Doheny-Adams, T., Hunt, L., Cameron, D.D. & Gray, J.E. (2015) Manipulating stomatal density enhances drought tolerance without deleterious effect on nutrient uptake. *The New Phytologist*, 208(2), 336–341.
- Hochberg, U., Degu, A., Fait, A. & Rachmilevitch, S. (2013) Near isohydric grapevine cultivar displays higher photosynthetic efficiency and photorespiration rates under drought stress as compared with near anisohydric grapevine cultivar. *Physiologia Plantarum*, 147(4), 443–452.
- Kage, H. (1997) Is low rooting density of faba beans a cause of high residual nitrate content of soil at harvest? *Plant and Soil*, 190(1), 47–60.
- Laucou, V., Boursiquot, J.M., Lacombe, T., Bordenave, L., Decroocq, S. & Ollat, N. (2008) Parentage of grapevine rootstock ‘Fercal’ finally elucidated. *Vitis*, 47(3), 163–167.
- Matimati, I., Verboom, G.A. & Cramer, M.D. (2014) Nitrogen regulation of transpiration controls mass-flow acquisition of nutrients. *Journal of Experimental Botany*, 65(1), 159–168.
- Ollat, N., Bordenave, L., Tandonnet, J.P., Boursiquot, J.M. & Marguerit, E. (2014, October) Grapevine rootstocks: origins and perspectives. In *International symposium on grapevine roots 1136* (pp. 11–22).
- Polley, H.W., Johnson, H.B., Tischler, C.R. & Torbert, H.A. (1999) Links between transpiration and plant nitrogen: variation with atmospheric CO₂ concentration and nitrogen availability. *International Journal of Plant Sciences*, 160(3), 535–542.
- Pons, T.L. & Bergkotte, M. (1996) Nitrogen allocation in response to partial shading of a plant: possible mechanisms. *Physiologia Plantarum*, 98(3), 571–577.
- Reynolds, M., Manes, Y., Izanloo, A. & Langridge, P. (2009) Phenotyping approaches for physiological breeding and gene discovery in wheat. *Annals of Applied Biology*, 155(3), 309–320.
- Rosssdeutsch, L., Schreiner, R.P., Skinkis, P.A. & Deluc, L. (2021) Nitrate uptake and transport properties of two grapevine rootstocks with varying vigor. *Frontiers in Plant Science*, 11(608), 813.
- Salazar-Tortosa, D., Castro, J., Villar-Salvador, P., Viñegla, B., Matias, L., Michelsen, A. et al. (2018) The “isohydric trap”: a proposed feedback between water shortage, stomatal regulation, and nutrient acquisition drives differential growth and survival of European pines under climatic dryness. *Global Change Biology*, 24(9), 4069–4083.
- Schmittgen, T.D. & Livak, K.J. (2008) Analyzing real-time PCR data by the comparative CT method. *Nature Protocols*, 3(6), 1101–1108.
- Schulze, E.D. & Bloom, A.J. (1984) Relationship between mineral nitrogen influx and transpiration in radish and tomato. *Plant Physiology*, 76(3), 827–828.
- Serra, I., Strever, A., Myburgh, P.A. & Deloire, A. (2014) The interaction between rootstocks and cultivars (*Vitis vinifera* L.) to enhance drought tolerance in grapevine. *Australian Journal of Grape and Wine Research*, 20(1), 1–14.
- Stevens, J., Faralli, M., Wall, S., Stamford, J.D. & Lawson, T. (2021) Stomatal responses to climate change. In: *Photosynthesis, respiration, and climate change*. Cham: Springer, pp. 17–47.
- Tandonnet, J. P., Cookson, S. J., Vivin, P. & Ollat, N. (2010). Scion genotype controls biomass allocation and root development in grafted

- grapevine. *Australian Journal of Grape and Wine Research*, 16(2), 290–300.
- Tanner, W. & Beevers, H. (2001) Transpiration, a prerequisite for long-distance transport of minerals in plants? *Proceedings of the National Academy of Sciences*, 98(16), 9443–9447.
- Taskos, D., Zioziou, E., Nikolaou, N., Doupis, G. & Koundouras, S. (2020) Carbon isotope natural abundance ($\delta^{13}\text{C}$) in grapevine organs is modulated by both water and nitrogen supply. *Oeno One*, 54(4), 1183–1199.
- Tombesi, S., Nardini, A., Frioni, T., Soccolini, M., Zadra, C., Farinelli, D. et al. (2015) Stomatal closure is induced by hydraulic signals and maintained by ABA in drought-stressed grapevine. *Scientific Reports*, 5(1), 1–12.
- Vandeleur, R.K., Mayo, G., Shelden, M.C., Gilliam, M., Kaiser, B.N. & Tyerman, S.D. (2009) The role of plasma membrane intrinsic protein aquaporins in water transport through roots: diurnal and drought stress responses reveal different strategies between isohydric and anisohydric cultivars of grapevine. *Plant Physiology*, 149(1), 445–460.
- Vandeleur, R.K., Sullivan, W., Athman, A., Jordans, C., Gilliam, M., Kaiser, B.N. et al. (2014) Rapid shoot-to-root signalling regulates root hydraulic conductance via aquaporins. *Plant, Cell & Environment*, 37(2), 520–538.
- Verdenal, T., Dienes-Nagy, Á., Spangenberg, J.E., Zufferey, V., Spring, J.L., Viret, O. et al. (2021) Understanding and managing nitrogen nutrition in grapevine: a review. *Oeno One*, 55(1), 1–43.
- Zamboni, M., Garavani, A., Gatti, M., Vercesi, A., Parisi, M.G., Bavaresco, L. et al. (2016) Vegetative, physiological and nutritional behavior of new grapevine rootstocks in response to different nitrogen supply. *Scientia Horticulturae*, 202, 99–106.

SUPPORTING INFORMATION

Additional supporting information can be found online in the Supporting Information section at the end of this article.

How to cite this article: Faralli, M., Bianchedi, P.L., Moser, C., Bontempo, L. & Bertamini, M. (2023) Nitrogen control of transpiration in grapevine. *Physiologia Plantarum*, 175(2), e13906. Available from: <https://doi.org/10.1111/ppl.13906>